Journal of Catalysis **189,** 326–338 (2000)
doi:10.1006/jcat.1999.2712, available online at http://www.idealibrary.com on IDEAL®

# Redox and Chemisorptive Properties of Ex-Chloride and Ex-Nitrate $Rh/Ce_{0.6}Zr_{0.4}O_2$ Catalysts

## 1. Effect of Low-Temperature Redox Cycling

Paolo Fornasiero,‡ Neal Hickey,‡ Jan Kašpar,‡,[1] Carlo Dossi,† Daniele Gava,‡ and Mauro Graziani‡

‡*Dipartimento di Scienze Chimiche, Università di Trieste, Via Giorgieri 1, 34127 Trieste, Italy; and* †*Dipartimento di Scienze Chimiche, Fisiche e Naturali, Università dell'Insubria, Via Castelnuovo, 7, 22100 Como, Italy*

Received May 14, 1999; revised September 20, 1999; accepted September 20, 1999

**The influences of low-temperature redox cycling and of the presence of chloride on the redox and chemisorptive properties of $Rh/Ce_{0.6}Zr_{0.4}O_2$ were investigated by means of volumetric hydrogen chemisorption, temperature-programmed reduction, and temperature-programmed desorption. This was achieved by conducting experiments on two samples of the material prepared from nitrate and chloride precursors. For the purposes of comparison, some parallel investigations were also conducted on the pure support. The results demonstrate that the interaction of $Rh/Ce_{0.6}Zr_{0.4}O_2$ with hydrogen is critically dependent not only on the presence of chloride but also on the specific treatments applied to the sample. The most important effect of chloride is that it inhibits the extent of vacancy creation at common operating temperatures of working three-way catalysts, thereby highlighting the unsuitability of chloride-based preparations for such materials. While some chloride can be removed under the low-temperature cycling conditions employed, the extent of this removal is small, and a lower degree of reduction was attained by the chloride sample throughout the series of experiments.** 

*Key Words:* **rhodium; ceria–zirconia; $CeO_2$–$ZrO_2$ solid solutions; chloride; redox properties; spillover; three-way catalyst; oxygen storage.**

### 1. INTRODUCTION

Primarily due to their application in automotive three-way catalysis there has been a growth in interest in ceria–zirconia mixed oxide solid solutions in recent years, as evidenced by their frequent appearance in both the scientific and the patent literature (1). These materials are being included in recent three-way catalyst formulations as oxygen storage components. The ability of a three-way catalyst to store oxygen under net oxidising conditions and release it under net reducing conditions—also known as its oxygen storage capacity (OSC)—has been regarded as being crucial to efficient three-way operation since the inclusion of ceria in formulations to achieve this purpose in the 1980s (2). In this function ceria–zirconia mixed oxides are considered to be superior to ceria and are therefore viewed as a more promising alternative. The importance of efficient oxygen storage behaviour has attained added significance in light of the proposal within EURO phase IV legislation to make it part of test procedures.

The advantages of ceria–zirconia materials over ceria stem largely from their enhanced reducibility and thermal stability. Although the exact behaviour depends on many factors, such as composition, texture, and pretreatment regimes, in general, it is true to say that in comparison to ceria these materials exhibit equal or enhanced reduction, which is the more difficult step of the redox process (3–6). Furthermore, they are able to maintain or even improve their reduction behaviour after high-temperature treatment, a step that effectively deactivates corresponding ceria materials.

A great deal of research effort has been directed toward understanding the reduction process over these oxides and their supported noble metal (NM) analogues. Of considerable importance in this regard is their interaction with $H_2$, which is the first step in the reduction mechanism. Interaction between the metal and the support has been shown to promote activation of hydrogen on the support surface, which is generally perceived to occur through spillover of hydrogen from the metal to the support. This results in lower reduction temperatures relative to those of metal-free materials. Accordingly, the hydrogen handling ability of the material at low and high temperatures is an important variable for these processes.

A further consideration in this regard is the ability of ceria-based materials to retain chloride from preparation procedures involving the use of a chloride precursor. The influence of support-retained chloride on the chemisorption and catalytic behaviour of supported metal samples has been well documented (7,8). To our knowledge no

[1] To whom correspondence should be addressed. E-mail: kaspar@univ.trieste.it. Fax: +39 040 6763903.



0021-9517/00 $35.00

consideration has been given to the influence of this variable on ceria–zirconia supported samples.

The effects of NM loading on the redox behaviour of $Ce_{0.5}Zr_{0.5}O_2$ have been recently addressed (9). This investigation concluded that the presence of supported Rh, Pt, or Pd strongly favours the reduction of the support compared with metal-free $Ce_{0.5}Zr_{0.5}O_2$. However, the microstructure of the support remained a crucial factor in determining the redox behaviour within this framework. The present work focuses on the influence of low-temperature redox cycling and the presence of chloride on the hydrogen chemisorption, redox, and catalytic properties of 0.5 wt% $Rh/Ce_{0.6}Zr_{0.4}O_2$. The results have been divided into two parts. Those in part 1 pertain to the influence of low-temperature redox cycling and the presence of chloride on chemisorption and redox properties. In the second part, the effects of chloride on the chemisorption, redox, textural, and catalytic properties after high-temperature redox cycling are addressed.

## 2. EXPERIMENTAL

### 2.1. Catalyst Preparation

In order to minimise the possible consequences of variations in preparation procedures, a common support—a $Ce_{0.6}Zr_{0.4}O_2$ solid solution—was synthesised from nitrate precursors by complexation of the cations with citrate as described previously (10). Water was used as a solvent. XRD and Raman investigation have confirmed that the preparation leads to the formation of a single phase. Two 0.5% $Rh/Ce_{0.6}Zr_{0.4}O_2$ catalysts were prepared with this material using $RhCl_3 \cdot 3H_2O$ and $Rh(NO_3)_3$ as metal precursors, employing the incipient wetness impregnation method. The samples were dried in an oven at 383 K for 12 h and then calcined at 773 K for 5 h. The sample prepared from the chloride salt is designated below as Rh/CeZr (Cl), while that prepared from the nitrate precursor is designed as Rh/CeZr (N).

### 2.2. Standard Cleaning Procedure

An *in situ* cleaning procedure was applied to each sample before any new experiment or series of experiments was performed. The procedure consisted of heating the sample in 5% $O_2$/Ar (25 ml $min^{-1}$) from room temperature to 900 K at a heating rate of 10 K $min^{-1}$, holding at that temperature for 0.5 h, and then cooling slowly, first in $O_2$/Ar to 373 K and finally to room temperature in He (11).

### 2.3. Analysis of Chloride Content

The chloride content of the samples was determined by potentiometric titration with $AgNO_3$ after the sample was dissolved in nitric acid (12). Details of this procedure will be reported elsewhere. An error of 5% was estimated. The analysis is specific to surface-retained chloride and does not return values for total chloride content. Aliquots of fresh and redox-cycled Rh/CeZr (Cl), aged according to the schedule described below, were analysed in this manner.

### 2.4. Volumetric Adsorption Experiments

$H_2$ chemisorption and BET surface area measurements were conducted using a Micromeritics ASAP 2000 analyser. *In situ* BET surface area measurements were carried out on the fresh samples (before and after cleaning) and after $H_2$ chemisorption measurements in order to follow any variation in this variable through the various procedures and therefore to facilitate comparison between the various runs. $H_2$ chemisorption experiments were conducted at 308 and 195 K. Consistent with previous work (9), the samples (ca. 1.0 g) were pre-reduced in a flow of $H_2$ (50 ml $min^{-1}$) at a heating rate of 10 K $min^{-1}$ up to the selected reduction temperature (423 K). After 2 h at this temperature, the samples were evacuated at 673 K for 5 h and cooled under vacuum to the adsorption temperature (195 or 308 K). Typically, an equilibration time of 10 min was employed. In certain cases a treatment procedure in $N_2$ (900 K, 5 h, 50 ml $min^{-1}$) was applied to samples prior to the commencement of chemisorption measurements. The samples were brought to the selected temperature in this flow of $N_2$ at a ramping rate of 10 K $min^{-1}$. Adsorbed volumes were determined by extrapolation to zero pressure of the linear part of the adsorption isotherm (100–400 Torr), and no corrections to eliminate the so-called reversible hydrogen adsorption were employed. A chemisorption stoichiometry $H : Rh = 1 : 1$ was assumed.

### 2.5. Temperature-Programmed Experiments

In all of the experiments described below high-purity gases were employed, which were further purified with water and oxygen traps.

*2.5.1. Temperature-programmed reduction/reoxidation.* Experiments consisting of temperature-programmed reduction (TPR–TCD)/reoxidation cycles were carried out in a conventional system equipped with a thermal conductivity detector. This system has been previously described (13). Characterisation was performed on 0.05 g of catalyst loaded onto a quartz bed in a U-shaped quartz microreactor. An additional layer of quartz was added on top to ensure thermal homogeneity of the gas passing over the sample. Analysis was performed under 5% $H_2$/Ar, with a flow rate of 25 ml $min^{-1}$ and up to 600 K (heating rate 10 K $min^{-1}$), at which temperature the samples were reduced isothermally for 15 min. After TPR, the samples were outgased under an Ar flow at 600 K for 60 min and ramped to 700 K (heating rate 10 K $min^{-1}$), before oxidation was carried out by a pulse technique to ensure a full oxidation

in the bulk of the solid solution (13). Pulses of $O_2$ (0.1 ml) were injected into the flow of Ar passing over the sample until complete recovery of $O_2$ was observed. This allowed estimation of the degree of reduction. In order to investigate the effects of this low-temperature cycling on the redox properties of the samples, the TPR/oxidation cycle described above was typically repeated up to eight times.

*2.5.2. Temperature-programmed reduction/desorption.* Temperature-programmed mass spectrometry (TPR–MS, TPD–MS) experiments were conducted using a VG Sensorlab quadropole mass spectrometer with POSTSOFT analysis software. Typically 0.2 g of sample was employed, in a U-shaped quartz reactor and encased in quartz as described above. The outlet of the reactor was connected via a heated capillary tube to the analyser head of the mass spectrometer. To investigate hydrogen uptake upon exposure at various temperatures, samples were cyclically subjected to the following procedure after the standard cleaning procedure:

(1) Reduction. Heated under flowing $H_2$ (5% in He, 30 ml $min^{-1}$) from room temperature to 423 K (10 K $min^{-1}$) and then reduced at that temperature for 75 min.

(2) TPD (Intermediate). Purged with He for 45 min at 423 K (60 ml $min^{-1}$) and subsequently heated to 873 K under the same He flow, maintained at this temperature for 30 min, and cooled to room temperature. TPD to 873 K was necessary to fully observe the eluted peaks.

(3) Adsorption. Exposed to $H_2$ (5% in He, 30 ml $min^{-1}$) at room temperature before the temperature was increased to the selected adsorption temperature (10 K $min^{-1}$), where exposure was continued for another 30 min. This was followed by cooling to room temperature under flow of the same gas. The temperatures of adsorption chosen were 308, 328, 348, and 373 K.

(4) TPD. Purged in He (60 ml $min^{-1}$) for 30 min to remove $H_2$ from the tubing and subsequently heated to 873 K under He flow (30 ml $min^{-1}$) with a heating rate of 10 K $min^{-1}$. The sample was maintained at the final temperature for 30 min.

(5) Reoxidation. After completion of the TPD experiment, the samples were cooled to 700 K, exposed to $O_2$ (5% in He, 30 ml $min^{-1}$), cooled to 423 K in this flow, and then cooled to room temperature in a flow of He (60 ml $min^{-1}$). After this the whole cycle could be repeated using a different adsorption temperature.

Samples obtained from these treatments are hereafter indicated as low-temperature (LT) cycled. A schematic representation of this procedure is given in Fig. 1. Unless specified above, an equilibration period of 30 min was employed each time a gas was passed over the sample before any ramping procedure was initiated.

Steps (1) and (2) were used respectively to ensure reduction of the sample and removal of any adsorbed hydrogen (in a similar manner to the chemisorption experiments). Steps (3) and (4) were the adsorption and desorption steps, respectively. As adsorption and desorption processes can be expected to occur at room temperature, the ramping procedure could only measure the amount of remaining adsorbed hydrogen, rather than simply being associated with adsorption at the specified temperature. Step (5) was designed to reoxidise the sample for the next cycle. This procedure was applied to both the support only and the Rh-loaded samples. In the former case, because of the dramatic differences in the redox behaviour induced by the presence of the metal, much higher reduction temperatures were required in step 1—623 and 873 K (step (2) consisted of either TPD to 873 K or switching to a flow of He at 873 K)—and a higher adsorption temperature in step 3—573 K (due

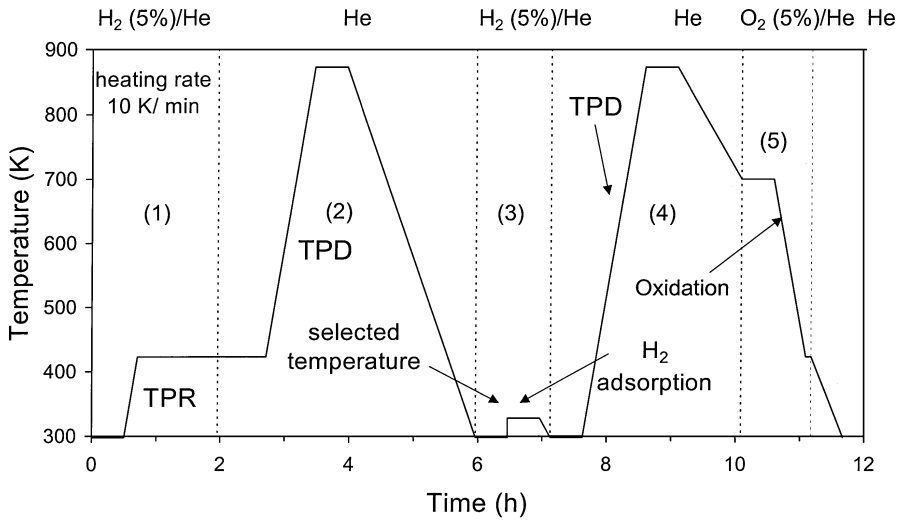


**FIG. 1.** Five-step low-temperature cycling procedure used to obtain experimental data.

to the activated nature of hydrogen adsorption on ceria–zirconia).

The information obtained during this overall procedure was three-fold. TPD–MS profiles were obtained during step (4). Exposure to $H_2$ during step (1) was monitored in order to address the issue of water formation during TPR (TPR–MS). Finally, the He treatment during step (2) was monitored to obtain information on hydrogen adsorption during the isothermal reduction at 423 K.

## 3. RESULTS

### 3.1. Standard Cleaning Procedure

The *in situ* cleaning procedure was deemed necessary in view of literature reports of the effect of easily removed impurities such as carbonates and nitrates on the behaviour of similar samples (14,15). Such impurities can, for example, lead to spurious TPR features, a method extensively employed in the present work. Temperature-programmed oxidation (MS) (not shown) demonstrated that no further $CO_2$ or NO evolution or oxygen uptake could be detected after this treatment, while the results of BET surface area analysis indicate that both of the fresh $Rh/Ce_{0.6}Zr_{0.4}O_2$ samples had BET surface areas of 38 $m^2\ g^{-1}$ before and after cleaning. Therefore, it can be concluded that the procedure cleans the sample, leaves it in a fully oxidised state, and does not affect its surface area.

### 3.2. Analysis of Chloride Content

The results of chemical analysis indicate a surface chloride content of 42 $\mu$mol $g^{-1}$ on fresh Rh/CeZr (Cl) and of 34 $\mu$mol $g^{-1}$ on an LT cycled sample. It should be noted that attempts to detect chloride removal under oxidising and reducing conditions by mass spectrometry failed, even on an analogously prepared 5% Rh-loaded sample.

### 3.3. Hydrogen Chemisorption

The results of hydrogen chemisorption experiments conducted on the two $Rh/Ce_{0.6}Zr_{0.4}O_2$ samples are detailed in Table 1. The undoped support showed negligible hydrogen chemisorption under the same experimental conditions.

*3.3.1. Rh/CeZr (N).* In the case of the fresh sample, significant spillover occurs at 308 K, leading to an apparent H/Rh ratio of 5.48. At 195 K this value decreases to 0.40. After LT cycling the uptake measured at 308 K (H/Rh = 5.40) is comparable to that obtained for fresh Rh/CeZr (N) at the same temperature, but the low-temperature value is higher than before, at 0.64. In an attempt to further address these observations, chemisorption experiments were conducted after both the fresh and cycled samples were subjected to a treatment in flowing $N_2$ at 900 K. Such a treatment has been demonstrated to significantly dehydroxylate similar samples and depress hydrogen spillover (9). The procedure results in decreased hydrogen uptake at 308 K for both fresh and LT cycled samples. However, the extents of hydrogen uptake are now considerably different (H/Rh = 1.99 vs 3.60). Furthermore, the procedure appears to have a minimal effect on the chemisorption values measured at 195 K.

The influence of hydrogen equilibration time was investigated in the case of the LT redox cycled sample after it had been subjected to the $N_2$ treatment. Doubling the equilibration time results in an increase in the hydrogen uptake

**TABLE 1**

**Volumetric Hydrogen Adsorption on $Rh/Ce_{0.6}Zr_{0.4}O_2$ Samples Pre-reduced at 423 K**

| Catalyst | Run | Pretreatment:[a] gas, temperature (K), time (h) | $H_2$ uptake[b] at 308 K ($\mu$mol $g^{-1}$) | $H_2$ uptake[b] at 195 K ($\mu$mol $g^{-1}$) | H/Rh[b] at 308 K | H/Rh[b] at 195 K |
|---|---|---|---|---|---|---|
| $Rh/Ce_{0.6}Zr_{0.4}O_2$ (N) | 1 | $O_2$ (5%)/He, 900, 0.5 | 133.4 | 9.8 | 5.48 | 0.40 |
| | 2 | $N_2$, 900, 5 | 48.2 | 9.8 | 1.99 | 0.40 |
| | 1 | LT redox cycled | 130.7 | 15.6 | 5.40 | 0.64 |
| | 2 | $N_2$, 900, 5 | 87.9 | 15.2 | 3.60 | 0.62 |
| | 3 | [d] | 142.8 | 16.1 | 5.88 | 0.66 |
| $Rh/Ce_{0.6}Zr_{0.4}O_2$ (Cl) | 1 | $O_2$ (5%)/He, 900, 0.5 | 24.5 | 9.4 | 1.01 | 0.38 |
| | 2 | $N_2$, 900, 5 | 16.1 | 9.4 | 0.66 | 0.38 |
| | 1 | LT redox cycled[c] | 23.2 | 11.6 | 0.96 | 0.48 |
| | 2 | $N_2$, 900, 5 | 15.2 | 11.6 | 0.63 | 0.48 |
| | 3 | [d] | 69.2 | 12.9 | 2.84 | 0.53 |

[a] Pretreatment applied before reduction at 423 K for 2 h. After reduction, samples were degassed in vacuum at 673 K for 2 h before chemisorption experiments.

[b] Hydrogen chemisorption measured at the indicated temperatures.

[c] Low-temperature redox cycled sample from TPR–MS experiments.

[d] Equilibration time was 20 min instead of the normal 10 min.

at 308 K (H/Rh = 3.6 vs 5.88). Because the value is higher than either of the previous results at 308 K, the possibility that spillover is incomplete in all of the measurements performed at 308 K cannot be excluded. Doubling the equilibration has no significant effect on the hydrogen uptake at 195 K.

*3.3.2. Rh/CeZr (Cl).* For fresh Rh/CeZr (Cl), at 308 K significantly lower chemisorption is evident than in the case of fresh Rh/CeZr (N) (H/Rh = 1.01 vs 5.48). At 195 K, however, the uptake recorded is similar to that observed for Rh/CeZr (N) (H/Rh = 0.40 vs 0.38). The qualitative trends of the data obtained for the LT cycled samples are the same as those observed for Rh/CeZr (N) in that uptake is unaffected at 308 K but very slightly (in the present case) larger at 195 K (H/Rh = 0.48). The effect of an $N_2$ treatment at 900 K was also investigated. At variance with Rh/CeZr (N), no difference between the extent of response of the fresh and LT cycled samples was found, as the results obtained at 308 K are marginally but similarly decreased. As before, the results obtained at 195 K remain unaffected. The influence of doubling the equilibration time on hydrogen chemisorption was also studied using the recycled Rh/CeZr (Cl) sample. This resulted in higher adsorption at both temperatures of investigation (H/Rh = 2.84 and 0.53 at 308 and 195 K, respectively).

### *3.4. Temperature-Programmed Reduction*

The results of a series of consecutive low-temperature TPR–TCD profiles of Rh/CeZr (N) and Rh/CeZr (Cl) are presented in Figs. 2a and 2b. In comparison with the TPR profile of the support, hydrogen uptake occurs at much lower temperatures (16). Previous reports have established that TPR of these materials to such temperatures results in bulk reduction of the support (17). The single hydrogen uptake peak for all profiles obtained from Rh/CeZr (N) (Fig. 2a) may be attributed to concomitant reduction of metal and support. In the case of Rh/CeZr (Cl) (Fig. 2b) two peaks are observed in the TPR of the fresh sample at 363 and 440 K. The first peak may be attributed to reduction of the supported metal oxide and the second to support surface/bulk reduction. An interesting feature of these profiles is that both samples exhibit lower temperature hydrogen uptake as a result of the first redox cycle. This results in a loss of resolution of the two peaks in the case of Rh/CeZr (Cl) (Fig. 2b). The peak maximum decreases from 385 to 355 K in the case of Rh/CeZr (N) sample and from 440 to 370 K in the case of Rh/CeZr (Cl). In subsequent profiles the positions of these maxima change very little for Rh/CeZr (N). However, an additional feature in the case of the Rh/CeZr (Cl) sample is the sharpness of the hydrogen uptake peak, a facet that appears only after the second TPR. The position of this sharp feature coincides with the position of the rhodium reduction peak in the initial TPR and may, in fact, be viewed

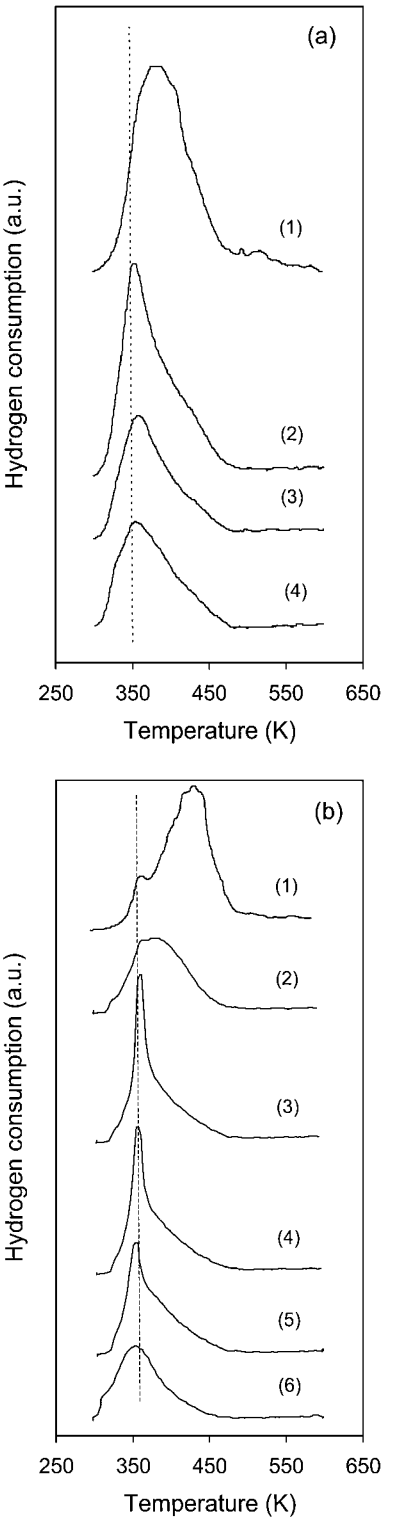


**FIG. 2.** Low-temperature TPR–TCD profiles of (a) $Rh/Ce_{0.6}Zr_{0.4}O_2$ (N), (1) fresh and (2)–(4) obtained on subsequent cycles, and (b) $Rh/Ce_{0.6}Zr_{0.4}O_2$ (Cl), (1) fresh and (2)–(6) obtained on subsequent cycles. The vertical lines indicate the position of bulk $Rh_2O_3$ reduction.

**TABLE 2**

**Oxygen Uptake at 700 K on $Rh/Ce_{0.6}Zr_{0.4}O_2$ (N) and $Rh/Ce_{0.6}Zr_{0.4}O_2$ (Cl) after Temperature-Programmed Reduction**

| Catalyst | Reduction treatment[a] (K) | No. of runs | $O_2$ uptake[b] ($\mu$mol $g^{-1}$) | $Ce^{3+}$ (%) | $Ce^{3+c}$ (%) |
|---|---|---|---|---|---|
| $Rh/Ce_{0.6}Zr_{0.4}O_2$ (N) | 600 | 1–8 | 455 | 43 | 39 |
| $Rh/Ce_{0.6}Zr_{0.4}O_2$ (Cl) | 600 | 1–8 | 361 | 34 | 30 |
| | 600[d] | 1 | 392 | 37 | 33 |

[a] The samples were repeatedly subjected to a classical TPR from room temperature up to the reported temperature and further reduced at that temperature for 15 min before the gas phase was desorbed in Ar for 60 min at 600 K and the temperature increased to 700 K for pulsed reoxidation.

[b] The reported data are average values. Standard deviation = $\pm 9$ $\mu$mol $g^{-1}$.

[c] Corrected assuming that the metal is fully reoxidised.

[d] Reduced at 600 K for 2 h.

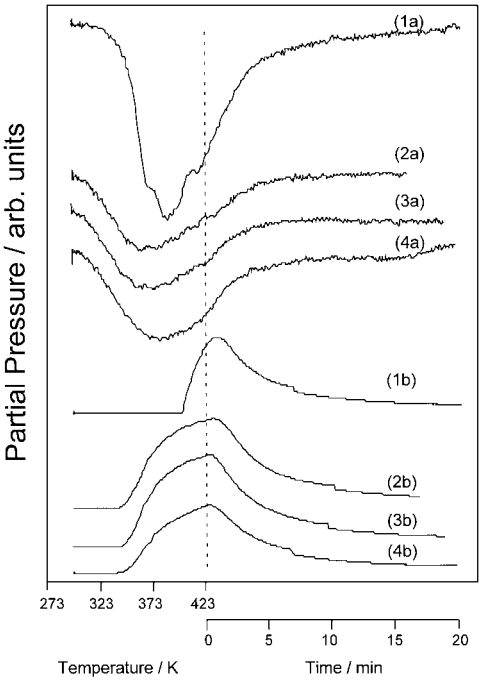


**FIG. 3.** Hydrogen uptake (traces a) and water evolution (traces b) in low-temperature TPR–MS profiles of $Rh/Ce_{0.6}Zr_{0.4}O_2$ (N), obtained during of step (1) of the five-step low-temperature cycling procedure (see Fig. 1). (1) Fresh and (2)–(4) obtained during subsequent cycles. The vertical line indicates a change in the *x*-axis from temperature ramping to isothermal reduction.

as being superimposed on the main $H_2$ uptake peak. This feature decreases slightly before disappearing on the sixth profile.

Table 2 shows the results of oxygen uptake measurements conducted after the TPRs discussed above. It should be noted that the results of TPD–MS experiments to be presented indicate that, due to adsorbed hydrogen, further reduction of the samples may occur upon increasing the temperature to 700 K after isothermal reduction. Therefore, the extent of reduction being reported is reduction at 600 K plus any additional reduction that occurs during the ramping procedure. Comparison of the oxygen uptake values reveals that there is a significantly smaller oxygen uptake for the Rh/CeZr (Cl) sample. This is despite the fact that 600 K, the upper-limit temperature of reduction, is well above the main hydrogen uptake exhibited during the TPR profile. Additional investigation, in which the reduction time at 600 K was increased from 15 min to 2 h, resulted in a higher degree of reduction of the Rh/CeZr (Cl) sample (Table 2). Nevertheless, even in this experiment the $O_2$ uptake is lower than that of Rh/CeZr (N).

Figure 3 shows a series of TPR–MS profiles obtained for the Rh/CeZr (N) sample (step (1), Fig. 1). For the first such TPR, effectively a fresh sample, hydrogen uptake starts significantly in advance of water production, indicating the occurrence of hydrogen storage effects. The maximum of hydrogen uptake occurs well before that of water production. In fact, the position of the hydrogen peak coincides quite well with that of the TPR–TCD (380 (MS) vs 385 K (TCD)). For the second TPR the position of the maximum of $H_2$ uptake shifts to lower temperature, reproducing the behaviour observed in the TPR–TCD. Water evolution starts much earlier, which is mainly responsible for a closer correlation between $H_2$ uptake and $H_2O$ formation across the temperature range. However, in terms of both the initial and maximum peak positions, a lag still exists between the two profiles, indicating that these variables are not directly linked. Further low-temperature redox cycling has little effect on the behaviour observed. Relative to the first low-temperature TPR, the $H_2$ uptake peak appears much smaller.

The results of an analogous series of TPR–MS experiments for the Rh/CeZr (Cl) sample are shown in Fig. 4. The general observations made with regard to the TPR of the fresh Rh/CeZr (N) sample and the changes that occur between this first and the second may also be made in this case. However, the fresh profiles do exhibit some significant differences in that for Rh/CeZr (Cl) the maximum of hydrogen uptake appears later. Furthermore, $H_2$ uptake is more gradual, although it begins at approximately the same temperature in both cases (ca. 323 K). As in the case of the fresh Rh/CeZr (N) profile, the initial hydrogen uptake does not correspond to sample reduction. However, it should be noted that water production at low levels may be difficult to detect, as indicated by the absence of a discrete peak due to $Rh_2O_3$ reduction. A final point to note with respect to comparison of the initial TPRs is that there is no significant difference in the temperature of vacancy creation. In subsequent profiles it can be seen that the sharp low-temperature uptake feature discussed in the case of the

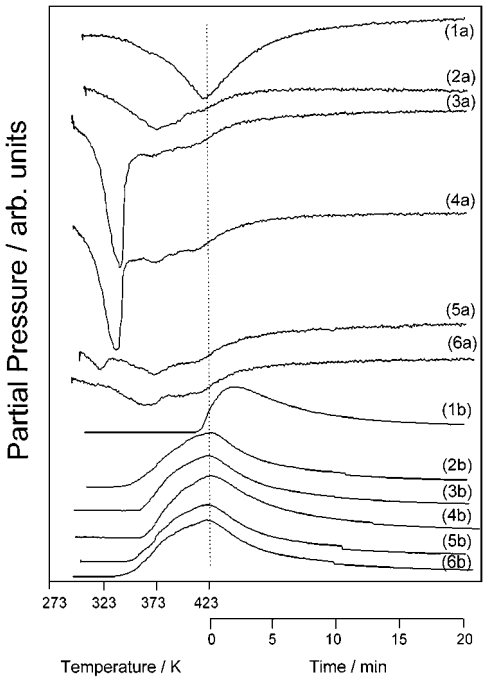


**FIG. 4.** Hydrogen uptake (traces a) and water evolution (traces b) in low-temperature TPR–MS profiles of $Rh/Ce_{0.6}Zr_{0.4}O_2$ (Cl), obtained during step (1) of the five-step low-temperature cycling procedure (see Fig. 1). (1) Fresh and (2)–(6) obtained during subsequent cycles. The vertical line indicates a change in the *x*-axis from temperature ramping to isothermal reduction.

TPR–TCD profiles also appears in these experiments and exhibits the same behaviour. This low-temperature uptake does not result in any concomitant $H_2O$ evolution.

As $H_2$ uptake at room temperature could not be addressed under the experimental conditions employed, semiquantitative analysis of the profiles is reported only for $H_2O$ produced. This analysis indicates that the total amounts of $H_2O$ desorbed across the full ranges of the profiles in Figs. 3 and 4 are similar ($\sim$250 $\mu$mol of $H_2O$ $g^{-1}$), except for the fresh samples ($\sim$165 $\mu$mol of $H_2O$ $g^{-1}$) due to nonattainment of the baseline in these experiments. Up to 423 K, there is an increase in the amount of water produced after the first cycle: from $\sim$46 to $\sim$90 $\mu$mol of $H_2O$ $g^{-1}$ in the case of Rh/CeZr (N), and from $\sim$28 to $\sim$80 $\mu$mol of $H_2O$ $g^{-1}$ in the case of Rh/CeZr (Cl).

### *3.5. Temperature-Programmed Desorption*

*3.5.1. Support.* Efforts to establish the desorption behaviour from the support were directed by the different redox behaviour of unloaded and Rh-loaded samples. The TPR profiles of the latter indicate that at 423 K both metal and support would have undergone considerable reduction. Much higher temperatures are required to achieve support reduction in the absence of the metal. For this reason two temperatures of pretreatment of the support were chosen, viz., 623 and 873 K. According to our TPR results (16), the former temperature corresponds to the beginning of the reduction range, while the latter is close the maximum of vacancy creation. These results are summarised in Fig. 5. After reduction at 623 K, TPD up to 873 K shows only $H_2O$ desorption (Fig. 5, traces 1a and 1b), indicating that only irreversible $H_2$ adsorption occurs on the sample at this temperature. As there was minimal $H_2O$ desorption during reduction at 623 K, the sample can therefore be considered to be only partially reduced. $H_2$ adsorption at 573 K on the sample thus treated is almost exclusively irreversible, as evidenced by the appearance of $H_2O$ only during the TPD (Fig. 5, traces 2a and 2b). It is of interest to note that $H_2O$ appears below 573 K, at which temperature the sample was exposed. After $H_2$ treatment at 873 K the sample is considerably reduced (confirmed by the prior TPR to 873 K), and, upon adsorption at 573 K, it exhibits a large $H_2$ desorption peak, centered at 840 K (Fig. 5, trace 3a), as well as a smaller water peak at 800 K (Fig. 5, trace 3b). Thus, there appears to be a difference between the $H_2$ adsorption on reduced and partially reduced surfaces (i.e., the initial

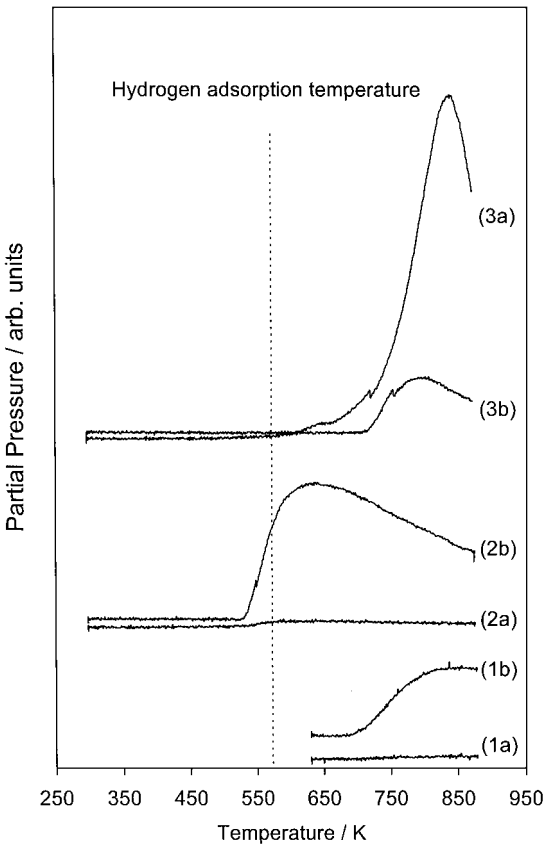


**FIG. 5.** Hydrogen uptake (traces a) and water evolution (traces b) during TPD from $Ce_{0.6}Zr_{0.4}O_2$ after various treatments: (1) TPD after isothermal reduction at 623 K; (2) TPD after hydrogen adsorption at 573 K on a sample reduced at 623 K; and (3) TPD after hydrogen adsorption at 573 K on a sample reduced at 873 K.

stages of reduction). The former situation is comparable to those of the Rh-loaded samples.

*3.5.2. Rh/CeZr (N).* TPD profiles obtained after exposure of Rh/CeZr (N) to $H_2$ at various temperatures are shown in Fig. 6. With respect to reversibly adsorbed hydrogen, two main desorption features are evident: a high-temperature peak near 550 K which remains in a fairly constant position after exposure at 308, 328, and 348 K, but which decreases slightly for the TPD after exposure at 373 K, and a low-temperature peak which shifts in position from 345 K after exposure at 308 K to 385 K after exposure at 373 K.

Semiquantitative analysis of these desorption profiles indicates that the total amounts of $H_2$ desorbed are 47, 80, 133, and 147 $\mu$mol of $H_2$ $g^{-1}$ at 308, 328, 348, and 373 K, respectively, indicating that the adsorption is an activated process. The baseline behaviour indicates that desorption is already taking place at the start of the profiles. In addition, the relative intensities of the two $H_2$ desorption peaks are affected by the exposure temperature, the low-temperature peak being favoured at higher adsorption temperatures. On the other hand, the amounts of $H_2O$ evolved remain roughly constant (between 31 and 47 $\mu$mol of $H_2O$ $g^{-1}$). Thus, a difference exists between behaviour of the amounts of reversibly and irreversibly adsorbed $H_2$. This could be due to the fact that the latter quantity is determined by the prior degree of reduction of the sample, which was reduced at 423 K before all TPD experiments.

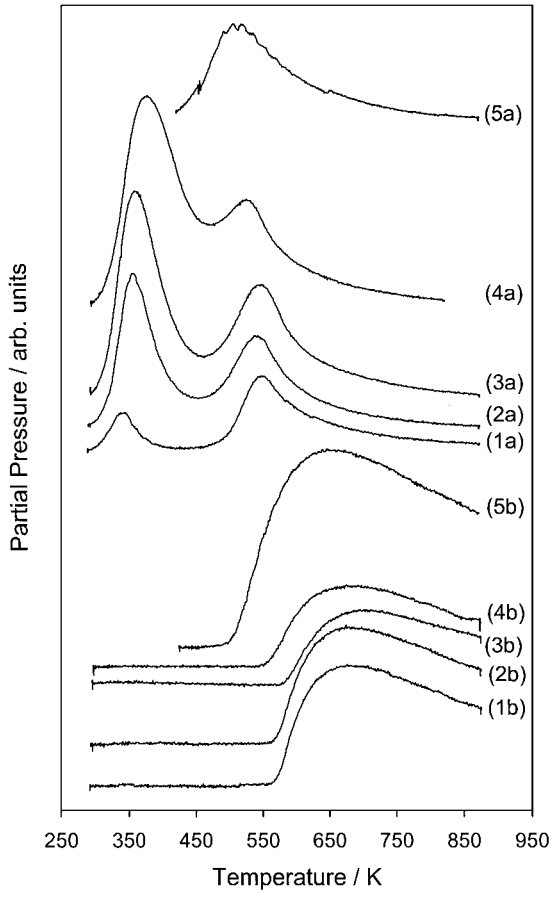


**FIG. 6.** Hydrogen evolution (traces a) and water evolution (traces b) during TPD from $Rh/Ce_{0.6}Zr_{0.4}O_2$ (N) after hydrogen adsorption at various temperatures, obtained during step (4) of the five-step low-temperature cycling procedure (see Fig. 1). Also included is a typical TPD after isothermal reduction at 423 K (step (2)). Temperature of $H_2$ exposure: (1) 308, (2) 328, (3) 348, (4) 373, and (5) 423 K (step (2)).

TPD profiles of the He treatment after isothermal reduction at 423 K (step (2), Fig. 1) were also recorded for both metal-loaded samples. These correspond to the adsorption behaviour at that temperature. Very similar behaviour was observed in all cases, and a typical profile is included in Fig. 6 (traces 5a and 5b). A single $H_2$ desorption peak is observable near 500 K. Thus, the decrease in position observed in the high-temperature peak after exposure at 373 K is continued upon exposure at the higher temperature. Due to the high initial temperature, the desorption behaviour at lower temperature is not apparent, so it is therefore not possible to tell whether increasing the reduction temperature is progressively resulting in a convergence of the peaks into a single peak and thus perhaps normalising the surface. These data also indicate that at 423 K both reversible and irreversible reduction occur on the sample and that further reduction occurs after the isothermal procedure.

*3.5.3. Rh/CeZr (Cl).* The results of an analogous series of $H_2$–TPD profiles from Rh/CeZr (Cl) are shown in Fig. 7. There are a number of qualitative similarities between the two sets of data: desorption occurs in two regions, and the amount of reversibly adsorbed hydrogen grows with increasing adsorption temperature. However, a significant difference relates to the position of the high-temperature peak. This is present at 640 K after exposure at 308 K and shifts to 550 K during successive runs. The final position is comparable to the position of this peak for all of the Rh/CeZr (N) experiments. $H_2O$ desorption also follows a general downward trend. The lower temperature peak behaves in the same way as for Rh/CeZr (N). It should also be noted that the first peak is broader than in the case of Rh/CeZr (N).

Semiquantitative analysis reveals that there is a lower amount of $H_2$ desorbed from Rh/CeZr (Cl) at equivalent temperatures in comparison with Rh/CeZr (N) (17,41,98, and 114 $\mu$mol of $H_2$ $g^{-1}$ at 308, 328, 348, and 373 K, respectively), while the $H_2O$ produced is 31 and 45 $\mu$mol of $H_2O$ $g^{-1}$, respectively, for fresh and cycled sample.

## 4. DISCUSSION

A four-step mechanism for the reduction of ceria, which can be extended to ceria–zirconia systems, has been

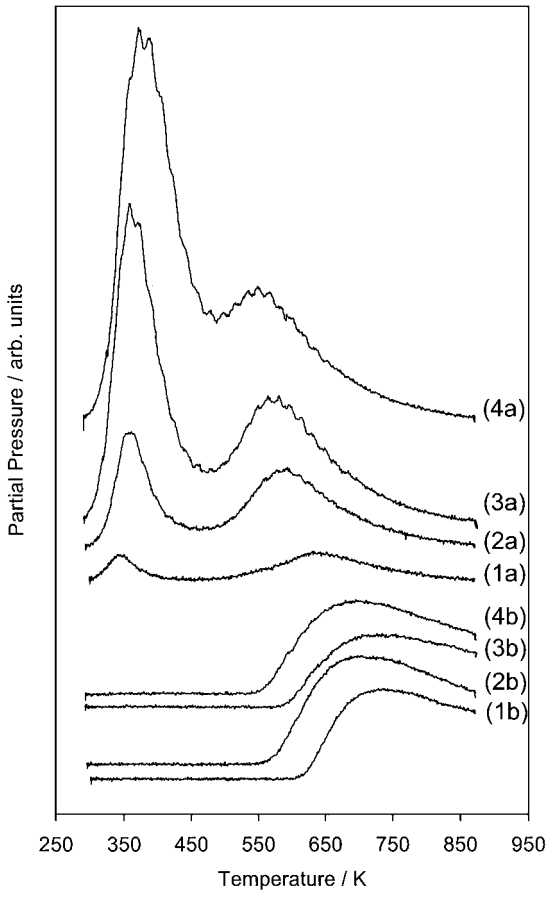


**FIG. 7.** Hydrogen evolution (traces a) and water evolution (traces b) during TPD from $Rh/Ce_{0.6}Zr_{0.4}O_2$ (Cl) after hydrogen adsorption at various temperatures, obtained during step (4) of the five-step low-temperature cycling procedure (see Fig. 1). Temperature of $H_2$ exposure: (1) 308, (2) 328, (3) 348, and (4) 373 K. In order to illustrate the profiles more clearly, these traces are plotted on a scale different from to that in FIG. 6.

proposed (18–20). This consists of adsorption of hydrogen leading to reversible reduction of ceria; vacancy creation, resulting in irreversible reduction of ceria; water desorption; and, finally, surface/bulk rearrangement through migration of vacancies to the bulk. However, within this scheme there are a number of aspects that have received little attention, most notably the mechanism by which water desorbs from the support (21). Upon doping of the support with a metal, greatly enhanced hydrogen uptake is observed at lower temperatures. Hydrogen spillover from the metal is generally held responsible for this observation. Spilled-over hydrogen may be stored on the surface as hydroxyls (7) or bronzes (22), create vacancies, or indeed be stored on the surface as water. A number of authors have concluded that the enhanced spillover in the presence of a NM results in lower temperature vacancy creation (1). Some authors cite the findings that the presence of rhodium facilitates easier removal of oxygen through oxygen migration from the support to the metal (23,24). The effectiveness of enhanced spillover in creating vacancies has been questioned by Bernal *et al.*, who have demonstrated that fewer vacancies are created in the case of $Rh/CeO_2$ than in the case of ceria upon isothermal reduction at 623 K (25). They suggest that in the former case the majority of $H_2$ is stored reversibly on the surface.

The present work addresses two closely related fundamental aspects of the redox behaviour of $Rh/CeO_2$–$ZrO_2$ systems, i.e., $H_2$ adsorption and vacancy creation. The results outlined present a comparison of the behaviour of two samples that differ in terms of the precursor used in their respective preparations. For the sake of convenience the following discussion will first deal with the response of the material designated Rh/CeZr (N) to the various methodologies used, followed by a comparison with that of the material designated Rh/CeZr (Cl). Throughout the following discussion it should be borne in mind that the surface area analyses demonstrated that the procedures used did not affect this variable.

### *4.1. Rh/CeZr (N)*

*4.1.1. Volumetric chemisorption.* Before a discussion of the effects of the pretreatments on H/Rh, it should be noted that the initial H/Rh of the two catalysts are identical when measured at 195 K. The choice of this temperature was based on previous investigation of $Rh/CeO_2$ which showed that at this temperature spillover is effectively arrested and such measurements should reflect the metal dispersion as, in that case, hydrogen should be Rh-adsorbed only (7,26). Since the presence of $ZrO_2$ in the support contributes to depressing the effectiveness of hydrogen spillover (27), we infer that $H/Rh = 0.38$–$0.40$ measured for the two fresh samples reflects the effective dispersion of the Rh particles. A standard reduction temperature of 423 K was chosen to ensure significant reduction of the rhodium present to rhodium metal. However, literature reports have indicated that complete reduction of the metal may not be achieved at this temperature, especially for the Rh/CeZr (Cl) sample (22,28). *In situ* surface area measurements conducted after each pretreatment procedure indicate that the low-temperature procedures employed did not affect this parameter.

Comparison of the results reported in Table 1 obtained from the fresh and LT cycled experiments reveals the following important findings: (i) At 308 K the H/Rh values are always higher that those measured at 195 K and strongly depend on the pretreatment, indicating contribution of hydrogen species spilt over the support. (ii) LT redox cycling leads to a higher uptake at 195 K compared to the fresh sample. (iii) After an identical dehydroxylation procedure there is a higher uptake at 308 K for the LT cycled sample, while the uptakes at 195 K are close to those obtained before the dehydroxylation procedure. (iv) When a longer

equilibration time was used the uptake at 308 K slightly increases for the LT cycled sample. (v) Qualitatively equal features, even if to a different extent, are observed in both Rh (N) and Rh(Cl) samples. This last point will be discussed later.

Let us first focus on the variation of H/Rh at 195 K with pretreatments (point (ii)). The degree of hydroxylation of the surface is often cited as a controlling factor in the spillover observed (29). Variations in spillover due to differences in the degree of hydroxylation may be proposed to partially explain this observation. Although some redispersion of the metal due to the reoxidation procedure cannot be excluded, this explanation is not entirely satisfactory as the conditions of recycling used were rather mild and were chosen specifically in order to minimise such effects. From points (ii) and (iii) above it appears that some spillover might occur after certain pretreatment procedures. However, such spillover seems to be minimal since both thermal pretreatment (iii) and doubling of the equilibration time (iv) only slightly affect the H/Rh at 195 K. Thus, the uptakes measured seem to reflect the metal dispersion also after redox cycling.

On the other hand, simply invoking the degree of hydroxylation cannot fully account for point (iii). The *in situ* reduction at 423 K applied to both fresh and LT cycled samples prior to chemisorption measurements should in theory result in similar degrees of hydroxylation, yet the significantly different uptakes at 308 K after the dehydroxylation procedure exist. A precise rationale of how this situation results from the starting materials is difficult to formulate. However, an idea that merits further investigation is that the spillover behaviour depends not only on the degree of hydroxylation but also on the type of hydroxyl groups formed. This is beyond the scope of the present investigation. Nevertheless, irrespective of the specific mechanism, these results clearly indicate that the interaction of these samples with hydrogen critically depends on the specific treatments administered to the sample.

*4.1.2. Temperature-programmed reduction.* The most significant aspects of the TPR–MS behaviour exhibited by Rh/CeZr (N) may be summarised in two observations: (i) there is significant low-temperature vacancy creation which is maintained through the LT cycling procedure, and (ii) after application of the first low-temperature cycle $H_2$ uptake shifts to lower temperatures while $H_2O$ formation begins earlier but the position of the peak maximum remains unaffected.

The first point is a well-established behaviour of metal-loaded ceria–zirconia mixed oxide materials and may be attributed to spillover of hydrogen from the metal to the support. In relation to the second point we infer the possibility that the majority of the hydrogen uptake observed during the first TPR which does not result in the subsequent TPRs has been shifted to room temperature, where it cannot be detected under the conditions of the experiments conducted. Although the amount of room temperature uptake for either sample could not be recorded, the initial behaviour of $H_2$ uptake demonstrates differences in hydrogen uptake capabilities after recycling. No uptake is evident in the TPR–MS trace below 323 K in the case of the fresh sample, whereas for the recycled samples uptake begins immediately. It is not unreasonable to suggest that some hydrogen uptake occurs before this initial temperature. Note that such spillover seems to be supported by the $H_2$ adsorption studies. The mechanism by which this would result in a lower temperature of water formation is not clear (vide infra), but clearly the initial vacancy creation is affected.

It is generally accepted that the presence of surface hydroxyls facilitates transport of dissociated hydrogen across the metal/support interface and across the surface away from the metal (29). An important chemical difference between these experiments is that for the first cycle the sample had not previously been exposed to $H_2$. During the first low-temperature TPR, reduction of the metal followed by spillover could significantly change the degree of hydroxylation of the surface. This may also explain the above-noted variations in vacancy creation: the earlier appearance of $H_2O$ is associated with surface hydroxyls, while the invariant position of the peak maximum is due to unaffected bulk reduction. A second possibility is that the reoxidation procedure does fully reoxidise the metal. Thus, before the first cycle all of the Rh should be present as $Rh_2O_3$ (cf. standard cleaning procedure) while after the first cycle the rhodium may be present in mixed states of a layer of easily reducible $Rh_2O_3$ on $Rh^0$, thereby leading to more facile spillover.

The reproducible behaviour after the first cycle indicates that the changes in the surface chemistry are reversible, but that the initial situation is not re-attained by the procedures used.

*4.1.3. Temperature-programmed desorption. Support.* On oxidised or partially reduced metal-free ceria–zirconia $H_2$ is exclusively adsorbed irreversibly, as water is the only desorption product. This is in agreement with the results of Bernal *et al.* in the case of ceria (25). On the other hand, a recent paper by Kondarides and Verykios in which TPDs from ceria were conducted under similar conditions indicated the occurrence of both $H_2$ and $H_2O$ formation (30). As previously mentioned, the temperature at which water appears is also of interest in that it is significantly lower than the temperature of the isothermal treatment applied to the sample in the reduction step. In addition, during the TPD experiment to 873 K after this isothermal reduction, further reduction was observed (which may be related to the capacity of the material for storage at that temperature). Thus, it is possible to further reduce ceria–zirconia at lower temperatures. Similar observations may be made after reduction at 873 K, where water again appears during

the TPD below the temperature at which the sample had been previously isothermally treated. In this case, however, reversible hydrogen adsorption accounts for the majority of the desorption observed, probably due to extensive reduction of the support during pretreatment.

*4.1.4. Rh/CeZr (N).* The presence of Rh results in the appearance of two new irreversibly adsorbed hydrogen peaks after exposure of the reduced samples to hydrogen at various temperatures. The degree of reduction of the sample means that the behaviour is comparable with that of ceria–zirconia reduced at 873 K. Two such regions of $H_2$ desorption from supported rhodium samples have been attributed to desorption from the bare support and metal-promoted desorption (25). In the present case, however, all of the observed desorption occurs at temperatures well below that of hydrogen desorption from reduced ceria–zirconia (Fig. 5), thereby indicating that the metal plays a crucial promotional role in all of the desorption observed, most likely through reverse spillover. This behaviour is in contrast with the findings of Kondarides and Verykios for 0.5% $Rh/CeO_2$; they found a high-temperature peak attributable to desorption of hydrogen from bare ceria (30). We therefore propose that the two peaks may be attributed to desorption from the metal and in the immediate vicinity of the metal and desorption from the support through back spillover. The near-metal region could include new sites created at the metal/support interface and support immediately adjacent to the metal particles. It seems unlikely that the first peak can originate solely from the metal in view of the fact that both peaks grow significantly throughout the series, which makes it impossible to distinguish the contribution from the metal in isolation. Such peak growth indicates an activated process. On the basis of the results available, within this proposed assignment the possibility of incorporation of hydrogen into the bulk and its subsequent desorption cannot be ruled out. These results therefore indicate an important difference between NM-loaded ceria and ceria–zirconia in that there is a much higher interaction between metal and support in the present case. The much lower adsorption temperatures required in this investigation are also suggestive of this conclusion.

Unlike the $H_2$ peaks, the $H_2O$ behaviour does not vary greatly with temperature as hydrogen adsorption temperature is increased. This again is in contrast with the findings of Kondarides and Verykios for 0.5% $Rh/CeO_2$; they found no water evolution during a TPD after hydrogen exposure at room temperature and the appearance of water at 673 K after exposure at 373 K (30). This may be indicative of the higher degree of reducibility of the ceria–zirconia support. Deep reduction of these materials is achieved more easily than that for comparable $Rh/CeO_2$ materials.

A notable difference between these results and those of the support is that in the present case water does not evolve until well above the temperature of isothermal reduction at 423 K. This might indicate that the full extent of reduction at 423 K is achieved, or at least the combination of this plus the additional reduction up to 873 K. Such a conclusion would represent an important difference between ceria-supported Rh and ceria–zirconia-supported Rh because in the former it has been shown that reversible adsorption predominates, albeit at a higher reduction temperature (25).

### *4.2. Rh/CeZr (Cl)*

A number of important general points, which must be remembered throughout the following discussion, should first be made. In addition to the equality of the surface areas throughout the procedures employed, the chemisorption results from the fresh samples at 195 K (Table 1) indicate equivalent dispersions. Furthermore chemical analysis demonstrates the presence of chloride on the fresh sample and its partial removal by the recycling procedure depicted in Fig. 1. Retention of chloride species appears to be a general property of the $Rh/CeO_2$-based systems (31), which is generally attributed to the formation of cerium oxychlorine species (32). In fact, on $Pt/CeO_2–Al_2O_3$ no appreciable amount of chloride was removed under calcination at 773 K (31). Interestingly, despite the relatively mild calcination temperature of the present catalyst, only a fraction of Cl remained at the surface, compared to the amount employed for catalyst preparation (146 $\mu$mol $g^{-1}$). Nevertheless, the chemical behaviour appears to be significantly affected.

*4.2.1. Volumetric chemisorption.* The main features of the Rh/CeZr (Cl) chemisorption results may be summarised as follows: (i) All the variations in H/Rh with pretreatment qualitatively reflect those of Rh/CeZr (N). (ii) Relative to Rh/CeZr (N), hydrogen uptake is dramatically inhibited at 308 K in all the cases. (iii) At 195 K, the value obtained for LT cycled Rh/CeZr (Cl) is somewhat lower than that of LT cycled Rh/CeZr (N).

The generally accepted view of the function of chloride in inhibiting spillover is that it is retained on the support (or substitutes for OH groups), thereby disrupting transport of hydrogen from the metal to the support (8) and transport of spilt-over hydrogen away from the metal across the support. Suppressed spillover due to the presence of chloride conveniently accounts for point (ii), although spillover has not been completely suppressed at 308 K, as evidenced by the higher H/Rh value (1.01) than that obtained at 195 K (0.38) (Table 1). Unpublished EXAFS investigation of a similarly prepared sample with a 5% Rh loading indicates that very little chlorine is associated with the metal. This is in accordance with the idea that transport of hydrogen from the metal is mainly affected by the presence of chlorine. If this idea is accepted, then the suggestion is that effects are occurring upon pretreatments that are almost independent of the presence of chloride (point (i)), except for the extent of variation of H/Rh (point (ii)). In fact, point (iii) could

suggest that some contribution of spillover can be responsible of the increase of H/Rh upon LT cycling, since higher H/Rh would be expected for Rh/CeZr (N) compared to Rh/CeZr (Cl) due to chloride species on the surface.

*4.2.2. Temperature-programmed desorption.* The presence of retained chloride has two main effects on the TPD behaviour of reversibly adsorbed hydrogen: (i) the amounts of desorbed $H_2$ are diminished after exposure at equivalent exposure temperatures, and (ii) the position of the high-temperature peak gradually decreases.

Point (i) is consistent with the idea that spillover is less efficient for the chloride sample during adsorption and constitutes evidence of the detrimental effect of the presence of chloride on the magnitude of spillover. Two possible explanations, not necessarily exclusive, may be put forward to explain the higher desorption temperature of the second peak in the fresh sample compared to that in Rh/CeZr (N). If, as outlined above, this desorption feature occurs through back-spillover then inhibition of this process by the presence of chloride would be expected. The second is that chloride retention creates an inhomogeneous oxide surface, which is in keeping with the EXAFS results, and that different energies are required to remove the adsorbed hydrogen.

The variation in behaviour with successive redox cycles is attributed to the observed partial removal of the chloride. Redox cycling has been previously demonstrated to have this effect on residual chloride (32).

*4.2.3. Temperature-programmed reduction.* Further evidence of the influence of retained chloride emerges from TPR behaviour. For both series of TPR experiments, a sharp peak superimposed on the main hydrogen uptake peak becomes evident. This peak coincides with the position of rhodium reduction and persists for several redox cycles (Figs. 2 and 3). In the case of the TPR–MS experiments, we can attribute this to a gradual decrease of the chloride content, which in turn permits enhanced low-temperature spillover to occur. As in the case of Rh/CeZr (N) this may be explained if $H_2$ uptake is displaced to room temperature, but gradually in the present case.

From the similar TPR behaviour it may also be concluded that the slightly different cycling procedure used in the case of the TPR–TCD experiments results in comparable levels of chloride removal. In this context, an important difference between the two samples is the degree of reduction attained after TPR to 423 K followed by TPD to 600 K, as measured by $O_2$ uptake at 700 K. The uptake measured is reproducibly 20% smaller in the case of Rh/CeZr (Cl). This corresponds to 187 $\mu$mol $g^{-1}$ of oxygen anions. Comparison of this value with the amount of chloride retained by the sample (34 $\mu$mol $g^{-1}$) suggests that substitution of oxygen by chloride is not the only significant factor in the decrease of uptake.

## 5. CONCLUSIONS

This paper has shown that the redox properties of $Rh/Ce_{0.6}Zr_{0.4}O_2$ display an extreme sensitivity to the pretreatment history of the sample and the presence of chloride. The extent of H activation is significantly higher in Rh/CeZr (N) compared to that in Rh/CeZr (Cl). Low-temperature redox cycling affects the spillover capabilities of both Rh/CeZr (N) and Rh/CeZr (Cl). This variable can also be altered by application of other thermal procedures. In comparison to $Rh/CeO_2$, $Rh/Ce_{0.6}Zr_{0.4}O_2$ exhibits a higher degree of interaction metal and support in terms of hydrogen spillover and vacancy creation. The TPD–MS suggests both that back-spillover is more facile and that vacancy creation is more extensive for $Rh/Ce_{0.6}Zr_{0.4}O_2$ (N). The presence of chloride affects the extent of vacancy creation in the sample. Redox cycling partially removes the chloride retained from preparation procedures, but a significant amount remains. Thus, chloride-based preparations, which are extensively used in industrial synthesis, have a detrimental effect on the OSC behaviour at normal operating temperatures of three-way catalysts.

## ACKNOWLEDGMENTS

University of Trieste, the Ministero dell'Ambiente (Roma), Contract No. DG 164/SCOC/97, CNR (Roma) Programmi Finalizzati "Materiali Speciali per Tecnologie Avanzate II, Contract No. 97.00896.34, and MURST (Roma) "Progetti di Ricerca di Rilevante Interesse Nazionale—1998" are gratefully acknowledged for financial support.

## REFERENCES

1. Kašpar, J., Fornasiero, P., and Graziani, M., *Catal. Today* **50**, 285 (1999).
2. Taylor, K. C., *in* "Catalysis—Science and Technology" (J. R. Anderson and M. Boudart, Eds.), Chapter 2. Springer-Verlag, Berlin, 1984.
3. Murota, T., Hasegawa, T., Aozasa, S., Matsui, H., and Motoyama, M., *J. Alloys Compd.* **193**, 298 (1993).
4. Ranga Rao, G., Kašpar, J., Di Monte, R., Meriani, S., and Graziani, M., *Catal. Lett.* **24**, 107 (1994).
5. Fornasiero, P., Balducci, G., Di Monte, R., Kašpar, J., Sergo, V., Gubitosa, G., Ferrero, A., and Graziani, M., *J. Catal.* **164**, 173 (1996).
6. de Leitenburg, C., Trovarelli, A., Zamar, F., Maschio, S., Dolcetti, G., and Llorca, J., *J. Chem. Soc., Chem. Commun.* 2181 (1995).
7. Bernal, S., Botana, F. J., Calvino, J. J., Cauqui, M. A., Cifredo, G. A., Jobacho, A., Pintado, J. M., and Rodriguez-Izquierdo, J. M., *J. Phys. Chem.* **97**, 4118 (1993).
8. Martin, D., and Duprez, D., *J. Phys. Chem. B* **101**, 4428 (1997).
9. Fornasiero, P., Kašpar, J., Sergo, V., and Graziani, M., *J. Catal.* **182**, 56 (1999).
10. Vidmar, P., Fornasiero, P., Kašpar, J., Gubitosa, G., and Graziani, M., *J. Catal.* **171**, 160 (1997).
11. Daturi, M., Binet, C., Lavalley, J. C., Vidal, H., Kašpar, J., Graziani, M., and Blanchard, G., *J. Chim. Phys.* **95**, 2048 (1998).
12. Kappers, M., Dossi, C., Psaro, R., Recchia, S., and Fusi, A., *Catal. Lett.* **39**, 183 (1996).
13. Fornasiero, P., Di Monte, R., Ranga Rao, G., Kašpar, J., Meriani, S., Trovarelli, A., and Graziani, M., *J. Catal.* **151**, 168 (1995).
14. Zotin, F. M. Z., Tournayan, L., Varloud, J., Perrichon, V., and Frety, R., *Appl. Catal. A Gen.* **98**, 99 (1993).

15. Perrichon, V., Laachir, A., Bergeret, G., Frety, R., Tournayan, L., and Touret, O., *J. Chem. Soc., Faraday Trans.* **90**, 773 (1994).
16. Fornasiero, P., Hickey, N., Kašpar, J., Montini, T., and Graziani, M., *J. Catal.* **189**, 339 (2000).
17. Di Monte, R., Fornasiero, P., Graziani, M., and Kašpar, J., *J. Alloys Compd.* **277**, 877 (1998).
18. El Fallah, J., Boujana, S., Dexpert, H., Kiennemann, A., Majerus, J., Touret, O., Villain, F., and Le Normand, F., *J. Phys. Chem.* **98**, 5522 (1994).
19. Bernal, S., Calvino, J. J., Cifredo, G. A., and Rodriguez-Izquierdo, J. M., *J. Phys. Chem.* **99**, 11794 (1995).
20. Fornasiero, P., Kašpar, J., and Graziani, M., *Appl. Catal. B Environ.* **22**, L11 (1999).
21. Overbury, S. H., Huntley, D. R., Mullins, D. R., and Glavee, G. N., *Catal. Lett.* **51**, 133 (1998).
22. Cunningham, J., Cullinane, D., Sanz, J., Rojo, J. M., Soria, J., and Fierro, J. L. G., *J. Chem. Soc., Faraday Trans.* **88**, 3233 (1992).
23. Jin, T., Okuara, T., Mains, G. J., and White, J. M., *J. Phys. Chem.* **91**, 3310 (1987).
24. Zafiris, G. S., and Gorte, J., *J. Catal.* **139**, 561 (1993).
25. Bernal, S., Calvino, J. J., Cifredo, G. A., Rodriguez-Izquierdo, J. M., Perrichon, V., and Laachir, A., *J. Catal.* **137**, 1 (1992).
26. Bernal, S., Calvino, J. J., Cifredo, G. A., Jobacho, A., and Rodriguez-Izquierdo, J. M., *J. Rare Earths* 838 (1991).
27. Fornasiero, P., Kašpar, J., and Graziani, M., *J. Catal.* **167**, 576 (1997).
28. Fajardie, F., Tempere, J. F., Manoli, J. M., Touret, O., Blanchard, F., and Djega-Mariadassou, G., *J. Catal.* **179**, 469 (1998).
29. Conner, W. C., and Falconer, J. L., *Chem. Rev.* **95**, 759 (1995).
30. Kondarides, D. I., and Verykios, X. E., *J. Catal.* **174**, 52 (1998).
31. Salasc, S., Perrichon, V., Primet, M., Chevrier, M., Mathis, E., and Moral, N., *Catal. Today* **50**, 227 (1999).
32. Fajardie, F., Tempere, J. F., Manoli, J. M., Djega-Mariadassou, G., and Blanchard, G., *J. Chem. Soc., Faraday Trans.* **94**, 3727 (1998).